Computers and Concrete, *Vol. 12, No. 2 (2013) 131-149*
DOI: http://dx.doi.org/10.12989/cac.2013.12.2.131

Seismic performances of RC columns reinforced with screw ribbed reinforcements connected by mechanical splice

Se-Jung Lee[1a], Deuck Hang Lee[2b], Kang Su Kim[2c], Jae-Yuel Oh[2d], Min-Kook Park[2] and Il-Seung Yang[*3]

[1]SEJIN Structure Construction Maintenance Co.,123-10 Nonhyun-dong, Gangnam-gu, Seoul 135-822, Korea
[2]Department of Architectural Engineering, University of Seoul, 90 Jeonnong-dong, Dongdaemun-gu, Seoul 130-743, Korea
[3]Department of Architectural Engineering, University of Dongshin, Daeho-dong 252, Naju, Chumnam, 520-714, Korea

(Received February 26, 2012, Revised June 4, 2012, Accepted January 17, 2013)

Abstract. Various types of reinforcement splicing methods have been developed and implemented in reinforced concrete construction projects for achieving the continuity of reinforcements. Due to the complicated reinforcement arrangements and the difficulties in securing bar spacing, the traditional lap splicing method, which has been widely used in reinforced concrete constructions, often shows low constructability and difficulties in quality control. Also, lap spliced regions are likely to be over-reinforced, which may not be desirable in seismic design. On the other hand, mechanical splicing methods can offer simple and clear arrangements of reinforcement. In order to utilize the couplers for the ribbed-deformed bars, however, additional screw processing at the ends of reinforcing bars is typically required, which often lead to performance degradations of reinforced concrete members due to the lack of workmanship in screw processing or in adjusting the length of reinforcing bars. On the contrary, the use of screw-ribbed reinforcements can easily solve these issues on the mechanical splicing methods, because it does not require the screw process on the bar. In this study, the mechanical coupler suitable for the screw-ribbed reinforcements has been developed, in which any gap between the reinforcements and sleeve device can be removed by grouting high-flow inorganic mortar. This study presents the uniaxial tension tests on the screw-ribbed reinforcement with the mechanical sleeve devices and the cyclic loading tests on RC columns with the developed coupler. The test results show that the mechanical sleeve connection developed in this study has an excellent splicing performance, and that it is applicable to reinforced concrete columns with a proper confinement by hoop reinforcement.

Keywords: sleeve; mechanical splice; seismic performance; screw ribbed reinforcement; grouting; reinforced concrete; column

∗Corresponding author, Professor, E-mail: yang1698@dsu.ac.kr
[a]Senior Structural Engineer, E-mail: mung222@sejinscm.com
[b]Ph. D. Student, E-mail: dklee@uos.ac.kr
[c]Asoociate Professor, E-mail: kangkim@uos.ac.kr
[d]Ph.D. Student, E-mail: hahappyppy@naver.com

http://www.techno-press.org/?journal=cac&subpage=8 ISSN: 1598-8198(Print), 1598-818X (Online)

1. Introduction

It is generally known that the lap splicing method is the most economical way to achieve continuity of reinforcements applicable to low-rise reinforced concrete (RC) buildings. As shown in Fig. 1(a), however, it is difficult to secure proper spaces for reinforcements due to the complicated rebar arrangements, thus the applications of lap splices to the medium height or high-rise buildings constructed in a seismic risk zone may result in low constructability and poor quality control. Also, because the lap-spliced regions are provided with twice as much rebar as required, if the lap splice length is estimated longer than required length, this lap-spliced region could be unexpectedly over-reinforced, and such excessive reinforcement is not desirable in terms of seismic design. Many researchers (Harajli 1994, Cho and Pincheira 2006, Kim *et al*. 2006, Ling *et al*. 2008a, 2008b, Chun *et al*. 2012, Chowdhury and Orakcal 2012, Ling *et al*. 2012, Lowes *et al*. 2012) reported that poorly-detailed lap-spliced zones showed poor seismic performances in their inelastic responses, such as excessive bond-slip, spalling of concrete cover, and reduced column strength, ductility and hysteretic energy dissipation capacity. It was also pointed out that the concrete cover losses due to corrosions in the reinforcements may cause a rapid reduction of the lap-spliced zone performance. Furthermore, in the case of large columns with the relatively large diameter reinforcing bars (for instance, over D35), the economic performance of the application of lap splice is considerably low. On the other hand, the mechanical splicing methods, as shown in Fig. 1(b), offers simple and clear reinforcement arrangements, and the longitudinal reinforcement ratio can be maintained equally through the member length. Furthermore, the axial resistance performances equal to the continuous rebar can be achieved easily. (ACI committee 439 1991, Hulshizer *et al*. 1994, Cagley and Apple 1998, ERICO Concrete Reinforcement Products 2006) However, as shown in Fig. 2(a), the most widely used parallel ribbed-deformed bars would require additional screw processing at the end of reinforcing bars connected by mechanical sleeve device. The use, including lack of workmanship in cutting the length of the such reinforcements would often result in insufficient connection performance between the prepared screw parts and the sleeve (Einea *et al*. 1995, Kim 2008, Belleri and Riva 2012, Ling *et al*. 2012, Metelli *et al*. 2011). Also, due to the inevitable gap between the reinforcements connected in the mechanical sleeve, performance degradations, such as slips of reinforcements from the sleeve device and corrosions, were often observed.

On the other hand, the screw ribbed reinforcements, shown in Fig. 2(b), do not need any additional processing or preparation at their ends for the application of mechanical splices to achieve the rebar continuity. In this study, therefore, a grouted-type mechanical coupler suitable for the screw ribbed reinforcement has been developed, which could increase the application of the screw ribbed reinforcement in construction. This study also aimed at verifying the mechanical and seismic performances of the developed coupler system. It should be noted that the developed coupler uses the inorganic mortar as a filler so as to improve the packing performance between the two splicing bars and sleeve (Einea *et al*. 1995, Kim 2008, Belleri and Riva 2012, Ling *et al*. 2012, Metelli *et al*. 2011). Fig. 3 shows the detailed construction sequence on the reinforcement continuity method developed in this study. The proposed method showed very excellent applicability in high-rise construction projects, and also the process of filling inorganic mortar with high liquidity was quite easily applied into the sleeve without using any large equipment. In this study, four reinforced concrete columns, to which the proposed splicing methods were employed, were designed to satisfy the structural detail conditions for intermediate moment-resisting frame specified in the current codes and tested to verify the practical performance of the developed coupler system. Test

variables were the location of mechanical sleeves and the concrete compressive strengths, and the RC column specimens were tested under reversed cyclic loading for the comparison of their seismic performances.

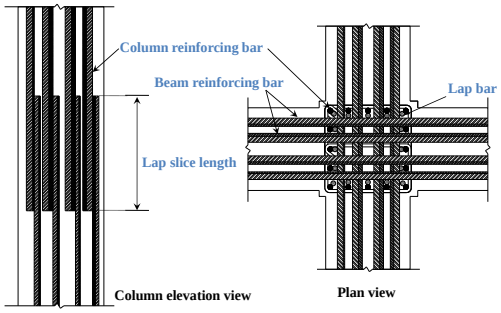

(a) An example of traditional lap slice

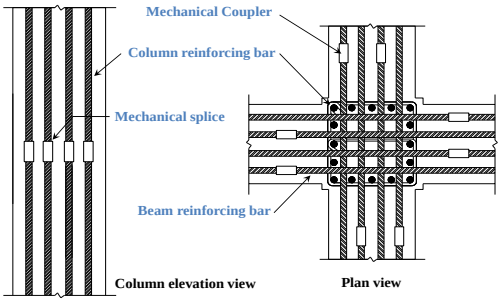

(a) Enhanced reinforcement splice by mechanical couplers

Fig. 1 Application of reinforcement splicing methods

(a) Typical parallel ribbed reinforcement

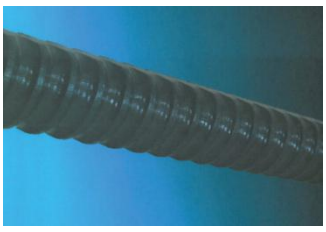

(b) Screw-ribbed reinforcement

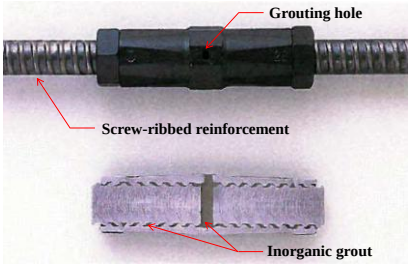

(c) Grouted mechanical splicing device and its sectional detail

Fig. 2 Rib shapes of reinforcements and developed mechanical splicing device

(a) Erection of pre-fabricated reinforcement cage

(b) Tightening the mechanical sleeve

(c) Grout work

Fig. 3 Description of construction sequences of the developed coupler

2. Experimental program

2.1 Specimens and material properties

Based on ACI318-11 (ACI Committee 318 2011) and the International Building Code (IBC 2012), the specimens were designed to satisfy the structural details for intermediate moment-resisting frame which are appropriate for the low to intermediate seismicity regions. As shown in Fig. 4 shows the actual prototype of column with half height, where, the total length of the specimens was 2,700 mm, and the net span length was 1,550 mm. All specimens had the rectangular section of 400 mm x 400 mm, and eight D25 steel bars were provided in longitudinal direction symmetrically. As shown in Fig. 4, D10 steel bars were used for the shear reinforcements (hoop reinforcements), which were placed at a 130 mm spacing in the end region of the specimen within 1.5 times the effective depth (d_s) from column-to-foundation connection, and at twice the end spacing in other regions. Also, the head stub and the foundation parts of the specimens were massively designed so that they could not affect the tested region during the reversed cyclic loading test. As shown in Table 1, the design compressive strengths of the concrete used in this

study were 30 MPa and 60 MPa, and their 28 day compressive strengths (f_c') were 36.8 MPa and 79.8 MPa, respectively. Shown in Table 2 are the grouting material properties used as the filler applied to the sleeve connector. The grout material is actually mass-produced in Japan and South Korea, and having high liquidity, it gives not only very excellent workability, but also considerably high compressive strength. The nominal yield strength of the longitudinal bars and the shear reinforcements used in the specimens were 500 MPa (SD500) and 400 MPa (SD400), respectively, and the longitudinal reinforcements were the screw-ribbed reinforcement, while the shear reinforcements were the conventional deformed reinforcement. In order to use the mechanical sleeve connection to the reinforced concrete columns designed in the seismicity regions, it should satisfy the seismic design provisions on mechanical splicing presented in the design codes (CSA 2004, KCI-M-07 2007, ACI Committee 318 2011), in which it is specified that the tensile strength of the reinforcement with mechanical couplers should provide over 125% of the nominal yield strength. If this condition is satisfied, Type-2 mechanical splice can be used, for instance, based on ACI318-11 design code. To examine whether the developed mechanical sleeve splice satisfies this regulation, as shown in Fig. 5 and Table 3, the uniaxial tension tests on the longitudinal screw-ribbed reinforcement with the couplers had been conducted. The test results in Fig. 5 and Table 3 showed that the tensile strengths of the specimens were over 130% of the nominal yielding strength. Therefore, the developed mechanical sleeve can achieve the type-2 splicing performance defined in ACI318-11 on special moment-resisting frame, which means that the coupler can be used to join reinforcing bars at any location within the member length including column-foundation connection. Also, as shown in Fig. 5, all reinforcements connected by the coupler tested in this study did not show any slippage between the sleeve and the reinforcements or bond failure of the grout filled in the sleeve. The connection failures were mainly due to fracture of reinforcing bars about 50 mm away from the sleeve, which shows excellent tensile performance of the developed sleeve connection.

Table 1 Compressive strength test results of cylinder specimen

Concrete type	7 day	14 day	28 day
30 MPa	18.1	27.6	36.8
60 MPa	53.5	64.1	79.8

Table 2 Material properties of inorganic grout

Compositions	CaO	61.5 - 64.5%
	SiO_2	18 - 20%
Material properties	specific surface area	6,000 - 8,000 cm^2/g
	Specific gravity	2.90 - 3.10
	flow *	120 - 200 mm (water-grout ratio 38%)
	Compressive strength**	More than 70 MPa

* Flow of grout material was estimated using simple flow test specified in JIS A 1108 with 20℃ temperature condition

** Under 20℃ water curing condition at 7 days after casting

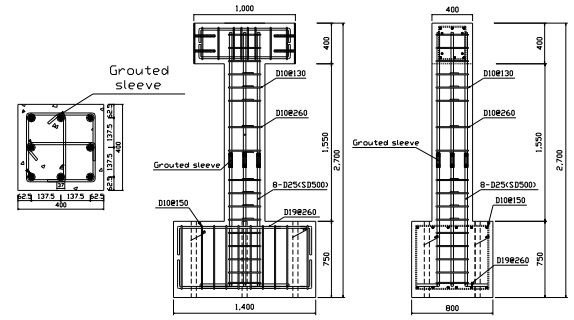

(a) Specimen C1

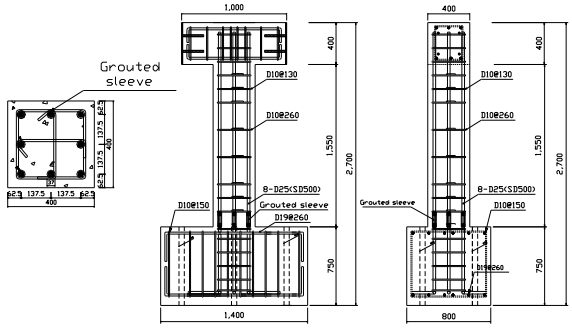

(b) Specimen S60J

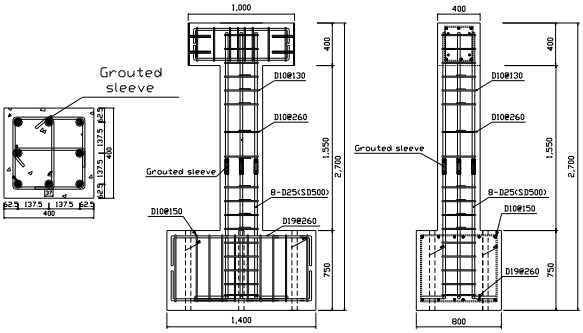

(c) Specimens S60D and S30D

Fig. 4 Dimensional details of test specimens

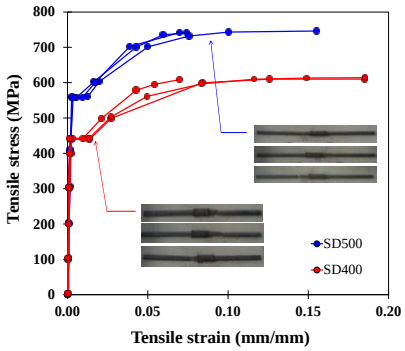

Fig. 5 Stress-train relationships of reinforcements with coupler

Table 3 Tensile test results of reinforcing bars

Type		Yield strength, f_y (MPa)	Tensile strength, f_u (MPa)	f_u / f_y ratio(-)	Percent elongation (%)
SD400	1	440.8	614.2	1.39	27.1
	2	441.8	608.8	1.38	27.2
	3	441.6	610.2	1.38	27.4
	Average	441.4	611.1	1.38	27.2
SD500	1	558.3	741.0	1.33	24.3
	2	561.4	742.0	1.32	23.9
	3	559.7	746.0	1.33	24.1
	Average	559.8	743.0	1.33	24.1

Table 4 Details and properties of specimens

Specimen name	C1 specimen	S60J specimen	S60D specimen	S30D specimen
f_c' (MPa)	79.8	79.8	79.8	36.8
Section type	Rectangular	Rectangular	Rectangular	Rectangular
Grouting	N.A.	○	○	○
* Splice	N.A.	M	M	M
** Location of splice devices	N.A.	Joint	$1.5d_s$	$1.5d_s$
b (mm)	400			
h (mm)	400			
*** ρ_s (%)	3.0%			
$A_{s,tot}$ (mm^2)	4053.6 (506.8 x 12EA)			
f_y, (MPa)	559.8			
f_u (MPa)	743.0			

* Mechanical splice

** Joint: slice is located in column-foundation connection, $1.5d_s$: slice is located at 1.5 from connection

*** $A_{s,tot}/bd$, where, b is width of cross-section, d is effective depth of cross section of column

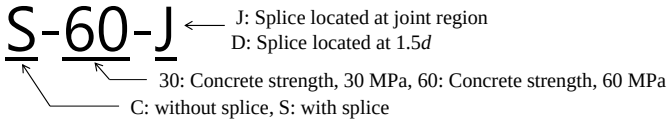

Shown in Fig. 5 and Table 4 are the dimensional details and material properties of the test specimens. As shown at the bottom of Table 4, the first letter of the specimen name indicates whether the mechanical splicing is applied or not (S: spliced rebar or C: continuous rebar); the second letter indicates the compressive strength of concrete (30: 36.8 MPa or 60: 79.8 MPa); and the third letter indicates the location of the mechanical sleeve (J: joint region or D: $1.5d_s$ from the column-foundation joint). The specimen C1, shown in Fig. 4(a), was a control test column without mechanical splice, and its compressive strength of concrete was 79.8 MPa. The specimen S60J, shown in Fig. 4(b), had the mechanical sleeve splices at the adjacent to the column-foundation connection while all other details are identical to the specimen C1. In the cases of the S60D and S30D specimens, as shown in Figs. 4(c) and (d), respectively, the mechanical sleeves were

installed at the section $1.5d_s$ away from the column-foundation connection to satisfy the type 1 splicing condition, as specified in ACI318-11, and their compressive strengths of concrete were 79.8 MPa and 36.8 MPa, respectively.

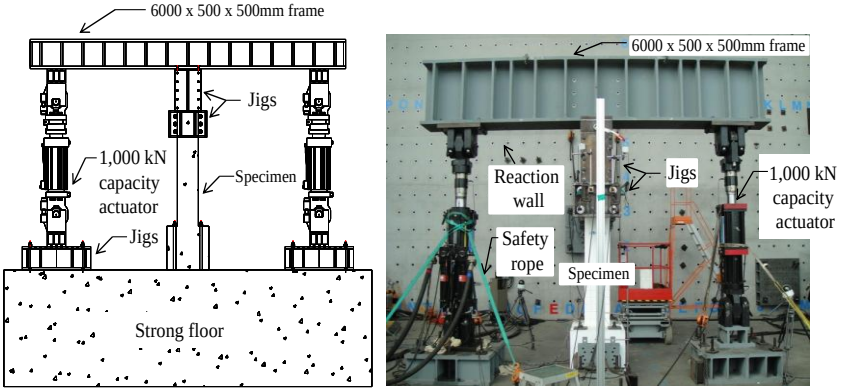

(a)N-S direction view

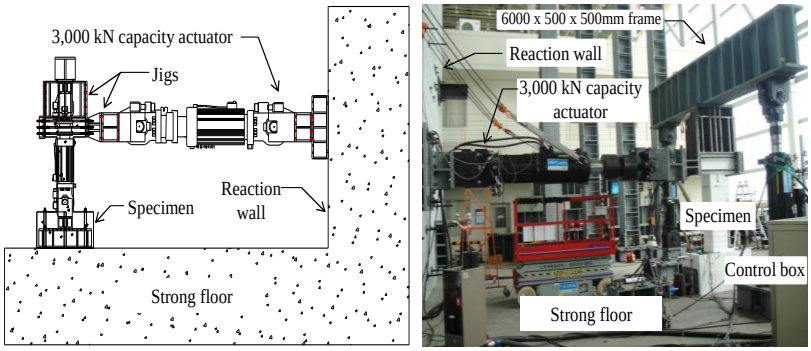

(b)N-S direction view

Fig. 6 Test set-up

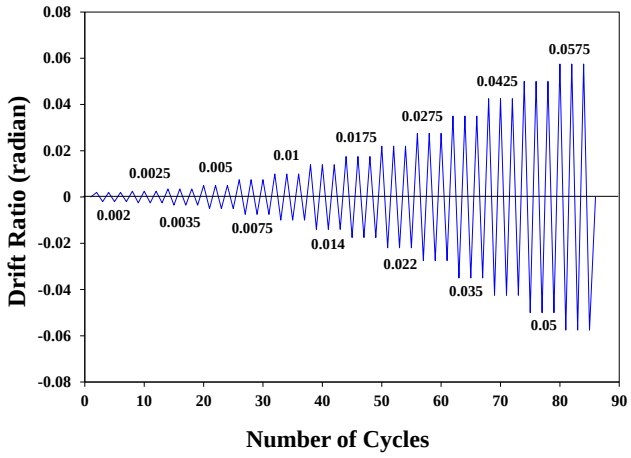

Fig. 7 Test profile of displacement controlled cycles

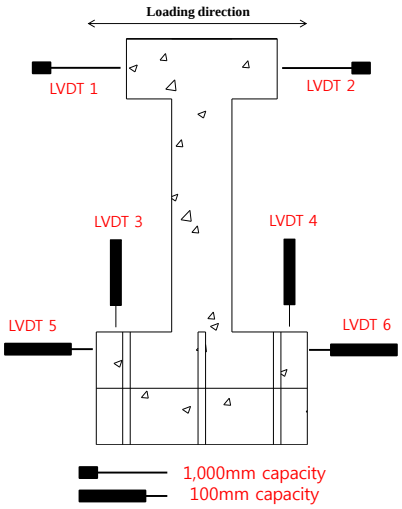

(a) LVDTs

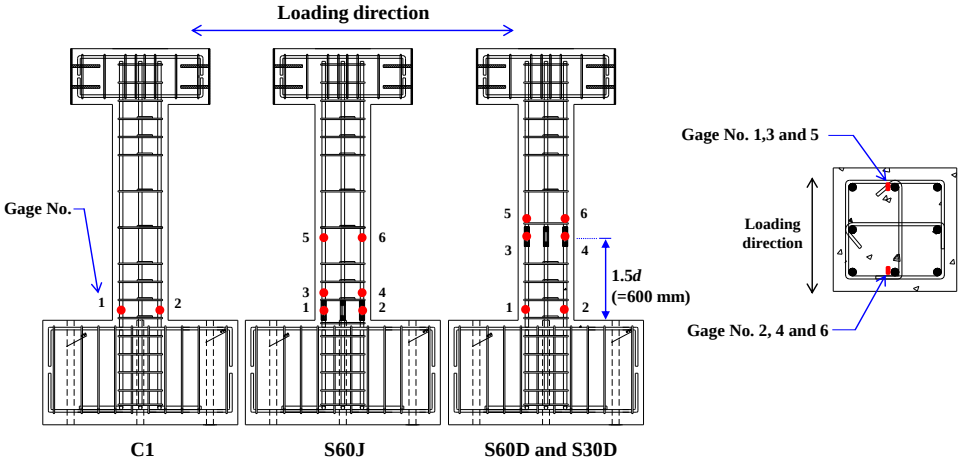

(b) Strain gages

Fig. 8 Locations of measurements

2.2 Test apparatus, loading conditions and measurements

In this study, lateral cyclic loads were applied to the specimens while maintaining the constant axial force level of $0.1 f_c' A_g$, where A_g is gross area of concrete section. The test setup of the experimental programme is shown in Fig. 6(a), where a 6000 x 500 x 500 mm frame was connected by bolts to the upper part of stub head of the specimens, and two actuators with 1,000 kN capacity were attached to the frame to introduce the constant axial force to the specimens. The axial load introduced to the specimens was monitored by the pre-installed load cell until the end of the testing, which was maintained within 5% variations. Once the target axial force is introduced,

as shown in Fig. 6(b), the lateral cyclic loads were applied by a 3,000 kN capacity actuator supported at the reaction wall, whose sequences are shown in Fig. 7. (ACI Innovation Task Group 1 and Collaborators, 2001) Fig. 8 shows the detailed descriptions on the measuring devices installed to the specimens, such as strain gages and LVDTs. As shown in Fig. 8(a), the average displacements, measured by the two LVDTs (LVDT 1 and LVDT 2) installed at the both sides of head stub of the specimen, were used to monitor the horizontal drift values. LVDT 3 and LVDT 4 were installed to monitor the movement of the specimen in upper direction; LVDT 5 and LVDT 6 were also installed to monitor the slippage between the specimen and the reaction floor in the loading direction. As shown in Fig. 8(b), strain gages were attached to the longitudinal reinforcements to measure the tensile and compressive strains of longitudinal reinforcements through all the positive and negative loading phases.

3. Test results

3.1 Load-drift responses and key observations

Fig. 9(a) shows the test result of the specimen C1, which is a control specimen without any splicing. In this control specimen, the screw-ribbed reinforcements made by SD500 steel were used as the longitudinal reinforcement, and its concrete compressive strength was 79.8 MPa. The load-drift response of the specimen C1 was a typical hysteretic behavior of reinforced concrete column. At 0.35% drift level, initial flexural cracks were observed, and their maximum width was about 0.05 mm. At 1.0% drift ratio, the longitudinal tensile reinforcements were yielded, the cracks propagated to the section about $1.5d_s$ away from the column-foundation connection, and concrete cover spalling was also observed at the corner of the column section. At 2.2% drift ratio, lateral resistance was reduced because concrete cover spalling on the compression zone of section was intensified at the adjacent to column-foundation joint, and shear cracks were also observed. Finally, at the second cycle of the 3.5% drift ratio, the crushing of concrete at the compression zone of section occurred simultaneously with the buckling of the longitudinal reinforcement, which led to the failure of the specimen with drastic reduction of load. As shown in Fig. 10(a), multiple shear cracks had also developed near and at ultimate state. The buckling of the longitudinal reinforcement was observed at the location about $1.5d_s$ away from column-foundation joint, in which the spacing of shear reinforcement at this location was larger as compared to spacing at bottom end of column specimen. This is believed to be due to the relatively smaller confining forces than that in the column-foundation connection region where smaller hoop spacing was provided. Also, the specimen C1 showed over 25% of loading reduction at 3.5% drift level, compared to the maximum load, which was somewhat below the seismic performance of special moment-resisting frame, as presented in the ACI T1.1-01 report (2001). As previously mentioned, however, all RC columns tested in this study were designed to satisfy the seismic performance for intermediate moment-resisting frame, and thus, it should be noted that they are not required to satisfy the criteria of the above-mentioned special moment-resisting frame.

Shown in Fig. 9(b) is the load-drift behavior of the specimen S60J that had the grouted-mechanical sleeve splice at the column-foundation connection, while all other details were identical to those of the specimen C1. The cracking strength, the initial stiffness, and the maximum load carrying capacity of the specimen S60J were almost identical to those of the specimen C1 that is the control specimen without any mechanical splice. As previously mentioned, the specimen C1

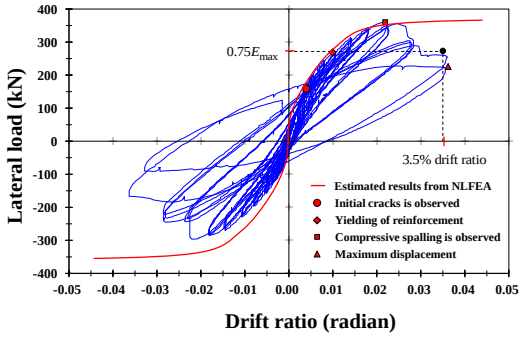

(a) Specimen C1

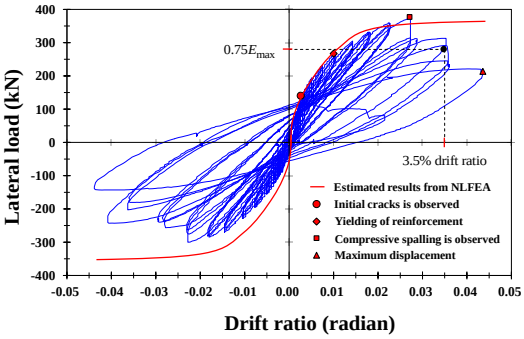

(b) Specimen S60J

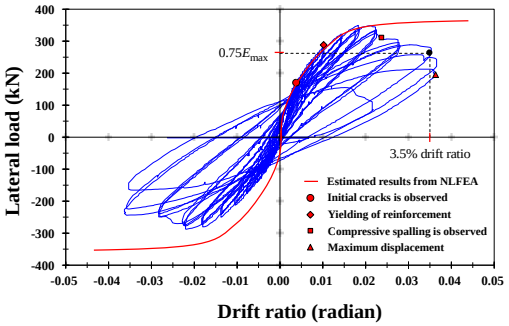

(c) Specimen S60D

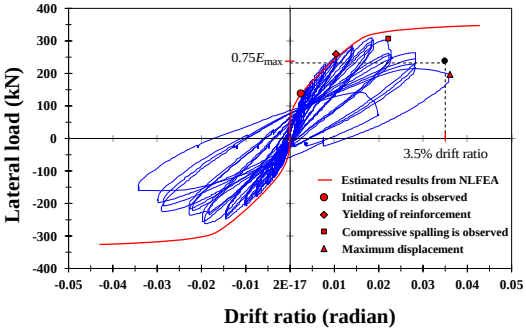

(d) Specimen S30D

Fig. 9 Comparisons of analysis results with experimental results

(a) Specimen C1

(b) Specimen S60J

(c) Specimen S60D

(d) Specimen S30D

Fig. 10 Photos of the test specimens at ultimate state

showed a significant load decrease at 3.5% drift level with crushing of concrete on compression side at the column-to-foundation connection. Although the specimen S60J also had a large amount of concrete cover spalling at the corner section adjacent to the column-foundation connection at the same 3.5% drift level, it had actually able to maintain 75% of the maximum load except at the third cycle of the drift. As shown on the left picture in Fig. 10(b), the specimen S60J failed at the second cycle of the 4.24% drift ratio, showing serious bond cracks developed along the longitudinal reinforcement and the crushing of concrete, and the crack patterns and the failure mode were almost identical to those of the control specimen C1. Shown on the right side of Fig. 10(b) is the S60J specimen in which concrete covers were removed intentionally after the test. The column-foundation connection with the grouted sleeve splice was properly fixed and not exposed outside due to the confinement effect of the closely arranged stirrups.

Fig. 9(c) shows the load-drift response of the S60D specimen, which had the mechanical sleeve splices at the section $1.5d_s$ apart from the column-foundation connection according to the type-1 connection condition as specified in ACI318-11, while all other details were identical to those of the specimens C1 and S60J. The overall behavioral characteristics, as well as the crack pattern, flexural strength, and deformation capacity, were very similar to those of the specimen C1. At 3.5% drift level, the shear reinforcements near to the sleeve section, i.e. $1.5d_s$ away from column-foundation connection (i.e., near the sleeve location), in which a smaller amount of the hoop reinforcement was provided than that in the connection region, were fractured and losing their anchorage, followed by buckling of the longitudinal reinforcement near the mechanical coupler devices. As shown in Fig. 10(c), and compared to the specimen S60J, more severe longitudinal

cracks were observed along the longitudinal reinforcement of specimen S60D, and as a result, the sleeves were exposed along the longitudinal cracks.

Shown in Fig. 9(d) is the cyclic response of the specimen S30D. The mechanical sleeve connections for achieving the reinforcement continuity were used in the same location as that of the specimen S60D. While the dimensional details were identical to the other specimens, the concrete compressive strength of specimen S30D was 36.8 MPa, slightly lower than the other specimens. The initial stiffness before the yielding of the longitudinal reinforcements was very close to that of the specimen C1, but due to the low compressive strength, shear cracks were observed at 1.4% drift level, and the maximum load carrying capacity was 85% of the specimen C1. At 2.2% drift level, the concrete in the compression region of the section at the column-foundation connection started to crush, showing a large part of concrete cover subjected to compressive stresses spalled from the specimen. As shown in Fig. 10(d), at 3.5% drift level, the test was finally terminated as a large amount of concrete covers fallen off, and the load was sharply reduced below 75% of its maximum load carrying capacity.

3.2 Evaluation of test results

Table 5 shows the comparison of the flexural strength between the test results and theoretical values estimated from the sectional analyses using the advanced sectional analysis program Response 2000 (Bentz and Collins 2001), and also ACI318-11. The actual material properties shown in Table 1 and Table 3 were used in the analysis. The calculated strengths of the columns were agreed well with the test results, giving a safety in a conservative manner. The column strengths showed the over-strengths ranged from 12% to 19% when estimated by ACI318-1 and at about 5% when analysed by Response 2000, which implied that the columns satisfied the acceptance criteria presented in the ACI T1.1-01 report (ACI Innovation Task Group 1 and Collaborators 2001).

The column specimens were also analyzed by the nonlinear finite element analysis program Vector2 (Wang and Vecchio 2009), and presented in Fig. 9 compared to the test results. All dimensional properties, material strengths, and boundary condition of column specimens shown in Figs. 5 and 6, and Table 4 were used in finite element analysis, and the constitutive models adopted in the finite element analysis model are shown in Table 6 in detail. Concrete body were modelled by four node quadlilateral elements, longitudinal steel reinforcements were modelled as axial truss elements, while transverse reinforcements were modelled in a smeared manner. The estimated monotonic lateral behavior of the column specimens were agreed well with the test results up to the peak strengths except post-peak behaviour, which is because the compressive spallings observed in the cyclic loading tests were not able to be captured by the finite element analysis program.

Table 5 Comparisons of test results to sectional analysis results

Specimen name	(1) ACI318-11(kN)	(2) R2K * (kN)	(3) Test results (kN)	(3)/(1)	(3)/(2)
C1	312.2	345.7	362.1	1.16	1.05
S60J	312.2	345.7	372.7	1.19	1.08
S60D	312.2	345.7	349.5	1.12	1.01
S30D	242.0	248.9	309.8	1.28	1.24

* R2K - the flexural capacity estimated by response 2000 program (Bentz and Collins 2001)

Table 6 Constitutive models used in nonlinear finite element analysis

Properties	Used models
Concrete compression pre-peak response	Hognestad parabola model
Concrete compression post-peak response	Modified park-kent model
Concrete compression softening	Vecchio 1992-a model
Concrete tension stiffening	No tension stiffening
Concrete tension softening	Not considered
Concrete tension splitting	Not considered
Concrete confined strength	Selby model
Concrete dilation	Variable - kupfer model
Concrete cracking criterion	Mohr-coulomb (Stress)
Concrete crack slip check	Vecchio-collins 1986
Concrete crack width check	Agg/2.5 max crack width
Reinforcement dowel action	Not considered
Reinforcement buckling	Refined dhakal-maekawa model
Bond model	Eligehausen model

3.3 Measured strains in reinforcements

Fig. 11 shows the strain responses of the longitudinal reinforcements measured from gage 1 and gage 2 installed at the column-foundation connection of the specimens C1 and S60J. In both specimens, the longitudinal reinforcement in the column-foundation connection yielded, and the screw-ribbed reinforcements showed sufficient bond performances after yielding. Therefore, it is considered that it has comparable bond performance with the general deformed rebar. In the case of the C1 specimen, the tensile reinforcement showed asymmetrical strain distributions under positive and negative loading phases. It is believed that this is due to the greater damages accumulated in the direction of the negative loading by crushing of the concrete. Also, when the longitudinal reinforcement underwent compressive strain, the strain values were measured smaller than those in tension. This can be explained that both the concrete and the longitudinal reinforcement had provided the compressive resistance to the compression zone with crack closing, whereas only the reinforcement had provided the tensile resistance to the tensile zone. Such a tendency was also observed from the test result measured from the gages 3 and 4 attached on the upper part of the sleeve in the specimen S60J as shown in Fig. 8(b). However, the strains measured from the gages attached on the sleeve devices showed symmetrical values as loading direction changed, which seems to imply that the compressive damage accumulated in concrete due to crack was in a similar level with the tensile damage in concrete at the location of the sleeve devices. Also, the strains of the sleeve device were larger than that in the rebar measured from the strain gages located in adjacent to the sleeve, which is basically because the sleeves were installed at the larger flexural moment region, compared to the location of the gages 3 and 4 attached on the rebar. On the other hand, it also signifies that there was no slip of reinforcements connected in the sleeve device, which means that the the grout filled inside the sleeve device provided proper confinement and worked well. In other words, this result shows excellent splicing performance of the developed mechanical coupler device. The measured strains from the specimens S60D and

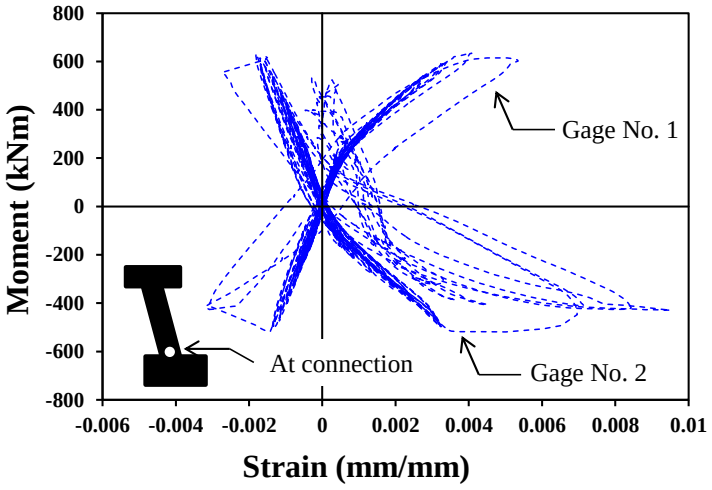

(a) Specimen C1

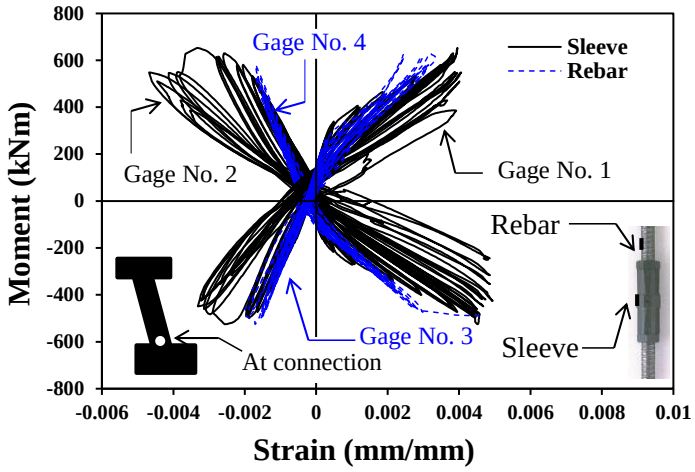

(b) Specimen S60J

Fig. 11 Strain responses of the specimens measured at connection region

S30D are shown in Fig. 12, however, showed different behavioral characteristics. The strains measured from the coupler, located at the section $1.5d_s$ away from the column-foundation connection, were larger under the tensile stresses region, as compared to the strain in compressive region. This is because more severe damages were occurred in the region near the coupler due to relatively smaller amount of stirrups compared to that in the column-foundation connection region.

3.4 Effect of location of mechanical splices and compressive strength of concrete

Shown in Fig. 13 is the comparison of the moment-rotation responses between the specimens S60J and S60D, from which the effect of the location of the mechanical splices on the cyclic responses of the RC columns can be observed. The specimen S60J with the sleeve devices near the

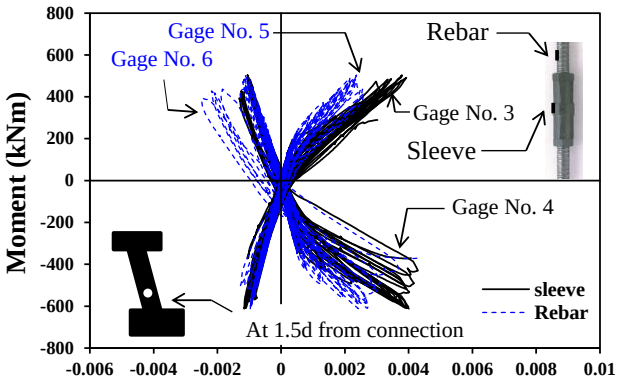

(a) Specimen S60D

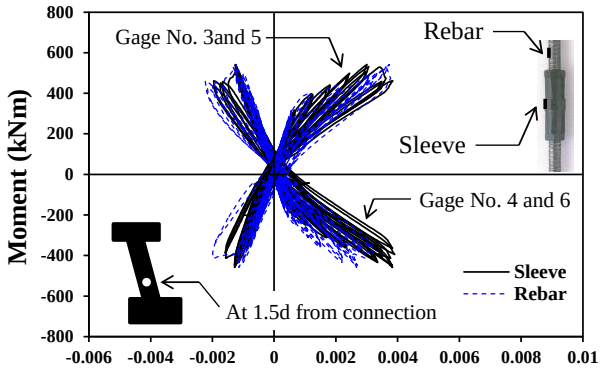

(b) Specimen S30D

Fig. 12 Strain responses of the specimens measured at $1.5d_s$ from connection region

column-foundation connection region showed higher strength and larger deformation capacity than the specimen S60D with the sleeve installed at the location $1.5d_s$ away from the connection.

The maximum load carrying capacity of the specimen S60J increased by 7% in the positive loading direction and by 5% in the negative loading direction, compared to that of the specimen S60D, whose difference is considered to be due to the difference in the confinement provided by the hoop reinforcement (Bechtoula *et al.* 2009). Thus, on the basis of this experimental result, in order to achieve enhanced strength and deformation capacity, it is advantageous to provide the sufficient amount of hoop to the column or to apply the mechanical splices to the column-foundation connection where the hoop spacing is the smallest.

Shown in Fig. 14 is the comparison of the test results of the specimens S30D and S60D, whose concrete compressive strength were 36.8 MPa and 79.8 MPa, respectively. As expected, the specimen S60D, whose concrete compressive strength was about twice the specimen S30D, had shown to have higher strength, but there was little difference in the deformation capacity. It can also be simply confirmed that the proposed mechanical sleeve connection is applicable to RC column cast with high-strength concrete as well as normal-strength concrete.

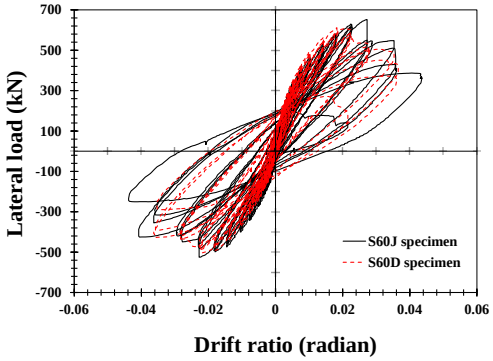

Fig. 13 Effect of splice location on cyclic responses of RC column

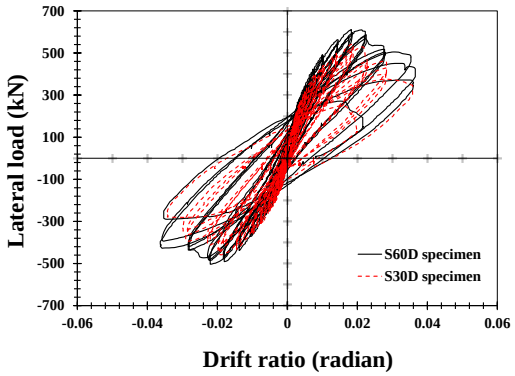

Fig. 14 Effect of compressive strength of concrete on cyclic responses of RC column

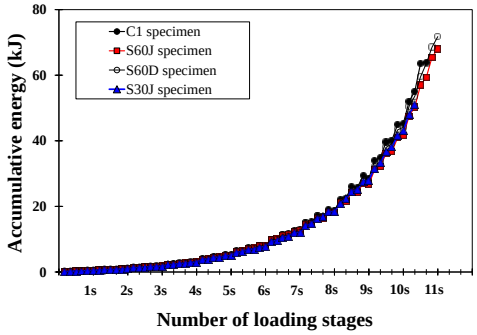

Fig. 15 Estimated accumulative energy dissipation of RC column specimens

3.5 Energy dissipation

Shown in Fig. 15 is the amount of cumulative energy dissipation of RC column specimens according to the loading stages. The specimens C1, S60J, and S60D have the same details, except for the location of the mechanical sleeve, and they all showed a similar amount of cumulative energy dissipation until the 10th loading stage (corresponding to 2.75% drift ratio), and little

difference after that. Even the specimen S30D, which had smaller concrete strength, showed a similar amount of energy dissipation capacity. Therefore, it is confirmed that the RC columns with the proposed mechanical sleeve have either similar or even improved seismic performance compared to the RC columns without splice.

4. Conclusions

To overcome the disadvantages of the traditional lap splicing method and existing mechanical splicing methods, this study developed a mechanical sleeve device appropriate to the screw- ribbed reinforcement formed in the rolling process at the production facility. The proposed mechanical sleeve connection is an inorganic mortar-grouted coupler developed to minimize the inevitable gap between the connecting reinforcements and sleeve. This study had conducted uniaxial tension tests on the reinforcement with the mechanical sleeve devices and the cyclic loading tests on RC columns with the developed coupler to verify the structural performances of the mechanical splices.

The results of uniaxial tension tests on the splices with the mechanical sleeve showed that their tensile strengths were over 130% of the nominal yield strength of steel reinforcement, which satisfied the type-2 splicing performance specified in ACI318-11 for the special moment-resisting frame, verifying that the mechanical sleeve connection developed in this study has an excellent splicing performance.

Also, the RC columns with the couplers showed similar or improved seismic performances compared to that with the continuous reinforcement, and it was shown that better seismic performances can be observed when the mechanical sleeve is confined by sufficient amount of hoop reinforcements.

Acknowledgments

The research program described in this paper was sponsored by the Tokyotekko Corporation, and authors also would like to acknowledge the contributions of the other investigators on this project, Jin-An Chung and Kyoung-Su Chung at the Research Institute of Industrial Science & Technology.

References

ACI Committee 318 (2011), Building Code Requirements for Structural Concrete and Commentary (ACI 318M-11), American Concrete Institute, Farmington Hills, 503.

ACI committee 439 (1991), “Mechanical connection of reinforcing bars”, *ACI Struct. J.*, **88**(2), 222-237.

ACI Innovation Task Group 1 and Collaborators (2001), Acceptance Criteria for Moment Frames Based on Structural Testing (ACI T1.1-01), American Concrete Institute, Farmington Hills, 10.

Bechtoula, H., Kono, S. and Watanabe, F. (2009), “Seismic performance of high strength reinforced concrete columns”, *Struct. Eng. Mech.*, **31**(6), 697-716.

Belleri, A. and Riva, P. (2012), “Seismic performance and retrofit of precast concrete grouted sleeve connections”, *PCI J.*, **57**(1), 97-09.

Bentz, E.C. and Collins, M.P. (2001), “Response 2000 ver. 1.1 user manual,”

http://www.ecf.utoronto.ca/~bentz/r2k.htm.
Cagley, J.R. and Apple, R. (1998), "Comparing costs — butt splices versus lap splices", *Concrete Int.*, **20**(7), 55-56.
CSA (2004), CAN3-A23.3-04: Design of concrete structures, *Can Stand. Assoc.*, Rexdale, Ontario, 213.
Cho, J.Y. and Pincheira, J.A. (2006), "Inelastic analysis of reinforced concrete columns with short lap splices subjected to reversed cyclic loads", *ACI Struct. J.*, **103**(2), 280-290.
Chowdhury, S.R. and Orakcal, K. (2012), "An analytical model for teinforced concrete columns with lap splices", *Eng. Struct.*, **43**(1), 180-193.
Chun, S.C., Lee, S.H. and Oh, B.H. (2012), "Simplified design equation of lap splice length in Compression", *Int. J. Conc. Struct. Mat.*, **4**(1), 63-68.
Einea, A., Yamane, T. and Tadros, M.K. (1995), "Grouted-filled pipe splices for precast concrete construction", *PCI J.*, **40**(1), 82-93.
ERICO Concrete Reinforcement Products (2006), Mechanical vs. Lap Splices in Reinforced Concrete Construction, http://www.erico.com/public/library/concrete/lt0983.pdf.
Harajli, M.H. (1994), "Development/splice strength of reinforcing bars embedded in plain and fiber reinforced concrete", *ACI Struct. J.*, **91**(5), 511-520.
Hulshizer, A.J., Ucciferro, J.J. and Gray, G.E. (1994), "Mechanical reinforcement couplings meet demand of strength and constructability", *Concrete Int.*, **16**(12), 47-52.
International Code Council (2012), International Building Code, 690.
KCI-M-07 (2007), Design Specifications for Concrete Structures, Korea Concrete Institute, 523.
Kim, H.K. (2008), "Structural performance of steel pipe splice for SD500 high-strength reinforcing bar under cyclic loading", *Archit. Res.*, **10**(1), 13-23.
Kim, T.H., Kim, B.S., Chung, Y.S. and Shin, H.M. (2006), "Seismic performance assessment of reinforced concrete bridge piers with lap splices", *Eng. Struct.*, **28**(6), 935-945.
Ling, J.H., Abd Rahman, A.B. and Mirasa, A.K. (2008a), "Performance of CS-sleeve under direct tensile load: Part I–failure modes", *Malaysian J. Civ. Eng.*, **20**(1), 89-106.
Ling, J.H., Abd Rahman, A.B. and Mirasa, A.K. (2008b), "Performance of CS-sleeve under direct tensile load: Part II–structural performance", *Malaysian J. Civ. Eng.*, **20**(1), 107-127.
Ling, J.H., Rahman, A.B.A., Ibrahim, I.S. and Hamid, Z.A. (2012), "Behaviour of grouted pipe splice under incremental tensile load", *Constr. Bldg. Mat.*, **33**(1), 90-98.
Lowes, L.N., Lehman, D.E., Birely, A.C., Kuchma, D.A., Marley, K.P. and Hart, C.R. (2012), "Earthquake response of slender planar concrete walls with modern detailing", *Eng. Struct.*, **43**(1), 31-47.
Metelli, G., Beschi, C. and Riva, P. (2012), "Cyclic Behaviour of a Column to foundation Joint for Concrete Precast Structures", *Euro. J. Env. Civ. Eng.*, **15**(9), 1297-1318.
Wong, P. and Vecchio, F.J. (2002), VecTor2 and Form Works User's Manual, Publication No. 2002-02, Department of Civil Engineering Publication, University of Toronto, 213.

CC